Institute of Paper Science and Technology
Atlanta, Georgia

IPST TECHNICAL PAPER SERIES

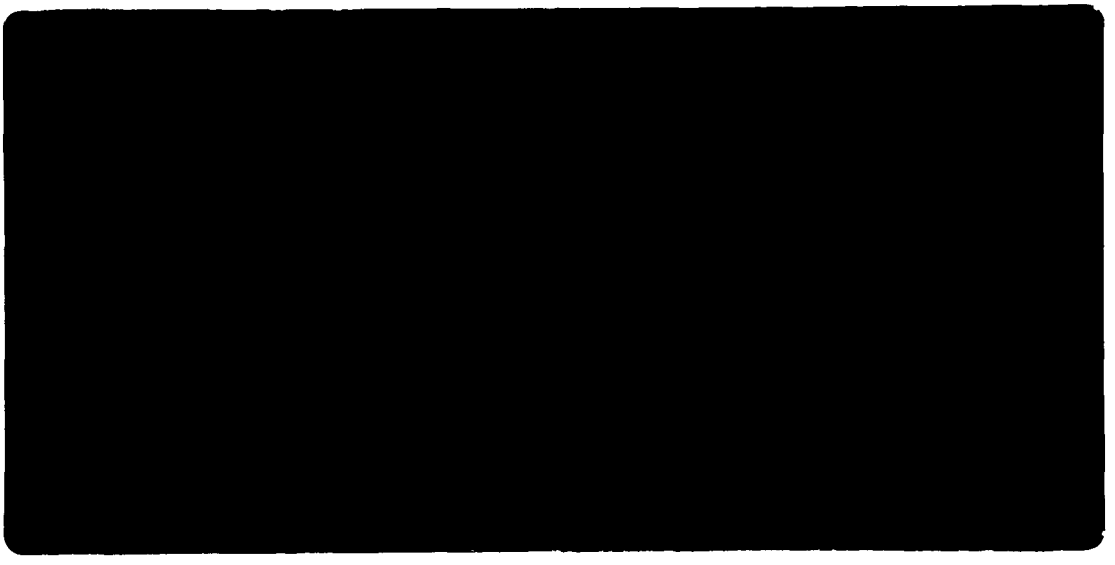

NUMBER 426

TRANSITION TO UNSTEADY FLOW IN A THROUGH-FLOW LID-DRIVEN CAVITY

J.D. BENSON AND C.K. AIDUN

MARCH 1992

Transition to Unsteady State Flow in a Through-Flow Lid-Driven Cavity

J.D. Benson and C.K. Aidun

Submitted to
Phys. Fluid A

TRANSITION TO UNSTEADY STATE FLOW IN A THROUGH-FLOW LID-DRIVEN CAVITY

J. D. Benson* and C. K. Aidun**

Institute of Paper Science and Technology
575 Fourteenth Street, N.W.
and
School of Mechanical Engineering,
Georgia Institute of Technology

Atlanta, Georgia 30318

ABSTRACT

A flush-mounted hot-film anemometer is used to investigate the transition to unsteady flow in a lid-driven cavity with a small amount of throughflow. The quantitative measurements with the hot-film probe confirm the transition from steady to time periodic state from our previous flow visualization studies and show a second transition in the primary state from time periodic to quasi-periodic flow and a transition to a state with broad band of frequencies typical of a chaotic state. From these results, we conclude that the transition to unsteady nonperiodic state in this system is through a torus bifurcation.

* Presently with Mead Central Research, Chillicothe, Ohio.
** Author to whom correspondences should be addressed.

1. INTRODUCTION

We are investigating the stability characteristics of flow in a lid-driven cavity (LDC) because of its importance as an ideal representation of coating [1], lubricating [2], and other manufacturing devices widely used in the industry. In addition to its industrial application, this device is important as a hydrodynamic system with ideal geometry and boundary conditions. In fact, it is frequently used as a benchmark for evaluation and examination of new computational algorithms. This system can be effectively used to study the physics of confined vortices in a simple geometry. A variation of this ideal system, where a small amount of fluid enters through the upstream edge of the bottom surface and leaves the cavity through the downstream lip, is termed a LDC with through flow.

Previously, we presented results from flow visualization studies of this system [3]. The primary steady state flow was shown to be nonunique and only one of the multiple steady state flow patterns which can stabilize in the cavity. It was also shown that the primary steady state destabilizes at the Cavity Reynolds number, $R = \rho l V/\nu$, at about 875 ($\pm$ 10%) and gives rise to a time periodic state. The velocity scale, V, and the length scale, l, are the lid velocity and the depth of the cavity, respectively. The aspect ratio of the cavity used in these studies is depth:width:span ratio equal to 1:1:3, as demonstrated in Fig. 1.

The time periodic state consists of spiral-shaped vortices superimposed on the steady state primary and secondary eddies forming traveling waves which appear at the symmetry plan, QRST, and approach the side walls where they disappear. As the Reynolds number increases, we have showed [3] that the dynamics become more complicated until the flow appears to be unsteady and nonperiodic. At this state, we observed mushroom-shaped vortices with rapid irregular motion. These structures appear to be very similar to the

Taylor-Gortler-like (TGL) vortices that Koseff and Street [4] observed in their study of turbulent flow in this system, which they show occurs at Re > 6000. These structures and the onset of turbulence in LDCs have also been studied by Prasad and Koseff [5], Freitas and Street [6], and other investigators as cited in Aidun et al. [3]. A number of major fundamental questions have remained unresolved. For example, the mode of transition from steady state to unsteady flow in this system is not well understood. In particular, it is not known whether the transition to turbulence is abrupt and through a *subcritical bifurcation*, such as in a Poiseuille flow, or low dimensional and ordered.

Our previous study [3] showed a transition from steady to time periodic state. In this study, we focus on the dynamics and stability of the flow at low to moderate Reynolds number. In particular, we will show the general mode of transitions from steady state to unsteady flow in this system. With the flow visualization technique used in our previous study [3], we were only able to capture the steady state and the time periodic flows. Flow visualization, although quite useful and effective as a first approach, could be deceptive particularly with unsteady flows.

To verify our flow visualization results and to learn more detail about the dynamics of the LDC flow, we used a hot-film anemometer to measure the wall shear rate as a function of the Cavity Reynolds number. We are not interested in magnitude of the wall shear rate but its dynamics which reflects the dynamical state of the flow. The hot-film probe is flush mounted with the cavity wall and, therefore, is considered to be a nonintrusive method of measurement.

In the next sections, we describe the experimental setup and procedure, results, and conclusions of this study.

2. EXPERIMENTAL SETUP AND PROCEDURE

We have used a hot-film sensor made of a thin metallic film. It is heated by an electric current and cooled by the incidental flow, which acts by virtue of its mass flux and its temperature [7]. The hot-film sensor, being sensitive to flow conditions, is used to measure the current (or resistance) and to determine the state of the flow. The resulting heat transfer between the hot-film sensor and the fluid is detected electrically as a function of the appropriate flow parameters [8].

In our experimental setup, the hot-film sensor is included in a Wheatstone bridge circuit. The offset voltage is amplified and fed back to the bridge to restrain the resistance changes of the hot-film sensor. A balanced bridge implies that the sensor resistance is constant, and therefore, the sensor temperature remains constant. We are, therefore, using a constant temperature anemometer [9].

Figure 2 shows a typical cylindrical FMHFA sensor and probe. The sensor, which is about 0.1 mm^2 in area, is flush with one end of the cylinder. Two platinum wires are connected to the ends of the flushed sensor and are enclosed inside of the cylindrical probe. These two wires extend out to the other end of the cylinder (right side of Fig. 2) and connect to a probe holder, which inputs a voltage signal across the Wheatstone bridge circuit.

The calibration of the FMHFA is usually made under steady flow conditions, and it is assumed that these calibrations will apply to quasi-steady [10] and to unsteady [11] flow conditions. Most hot-film anemometers are calibrated using steady Couette flow [12,13], where the stationary inner cylinder holds the probe and measures representative results for

shear stresses. The known shear stress of the fluid is then correlated and plotted versus the hot-film sensor readings.

Another method for calibrating the FMHFA is using the flow in a pipe. This technique is used by a number of investigators [14,15] and in our study, as well. In this case, the hot-film sensor is mounted flush with the inside tube wall of a long pipe. The flow in the test section is steady and fully developed. The shear stress is proportional to the pressure difference across the pipe, so the hot-film sensor reading is plotted versus the shear stress at the wall.

The FMHFAs are designed to be mounted flush with a surface or wall, where the flow is perpendicular to the axis of the probe body. It has been found that there will be as much as a 20% deviation in the hot-film anemometer bridge voltage with a change in probe position of 9% of the probe diameter from the wall. This could result in a 50% error in computed wall shear stress [15]. Therefore, it is of extreme importance to position the hot-film sensor as flush with a wall or surface as possible.

The necessary equipment used in calibrating the hot-film anemometer consists of an 11-foot, 3/4-inch diameter plexiglass pipe mounted on a flat surface. According to Langhaar [16] a fully-developed flow is established at $L = 0.057(Re)d$, where Re is the Reynolds number, and d is the pipe diameter. We allow an entry length of four feet before the first pressure transducer. The length between the two pressure ports is five feet. A pressure differential transducer used in this experiment provides a DC output voltage linearly proportional to the applied pressure. The FMHFA is placed halfway between the two pressure ports. The hot-film sensor, which is perfectly flush with the inside tube wall, is .127 by 1.016 mm in size. The output signal from the hot-film sensor is received by a

constant temperature anemometer which is then transmitted into a voltage signal and recorded by a data acquisition system.

In our calibration setup, the heat transfer between the hot-film sensor and the fluid is detected electrically as a function of shear stress. The constant temperature anemometer system operates on a +15 VDC (.7 amps) power supply. The probe, which holds the hot-film sensor and is 3.2 mm in O.D., is designed to be mounted flush with a surface or wall, where the flow is perpendicular to the axis of the probe body. The data collected from the hot-film sensor are recorded in volts with a data acquisition system connected to an IBM-PC. During the calibration experiment, the pressure difference across the pipe and the shear stress reading from the hot-film anemometer are recorded during each change in temperature of the fluid. The temperature of the fluid is increased from 20º C to 25 º C, and Δp readings are taken with every 0.2 º C increase in temperature. Since the hot-film sensor is very sensitive to temperature changes, a thermistor was installed next to the probe. Thus, the data acquisition system collects three parameters for the calibration setup -- the hot-film sensor signal, temperature, and pressure difference.

After all readings are taken, the actual shear stress is calculated and plotted versus the hot-film sensor reading. The results show that as the temperature increases shear stress decreases.

We have used the hot-film anemometer technique for measurements of the flow characteristics in a through-flow cavity. Mounted flush with the inside wall of the cavity, the probe and thermistor are both installed adjacent to each other. The quantitative data analysis also includes the flow rate feeding into the cavity. Using a data acquisition system, all of these parameters (temperature, flow rate, hot-film sensor) are collected at sampling rates of 10 Hz and 100 Hz.

Starting at the Reynolds number of about 200, the data are collected by the data acquisition system in increasing Re intervals of about 30 until Re reaches about 1300. Viscosity and fluid temperature readings are both taken at every interval in the Reynolds number range of 200 to 1300. After each experimental run, the data are analyzed to establish the state of the flow.

3. RESULTS

The first part of the experiments was to determine the sensitivity of the hot-film anemometer to the periodic fluctuations in the flow. As indicated in the last section, we constantly monitored the flow rate with an accurate flowmeter. The flow rate always shows slight fluctuations due to the transients in the pump. Although the magnitude of this fluctuation is very small compared to the fluctuations caused by flow instability, nevertheless, the hot-film probe can capture the behavior of the throughflow. Scaling the flow rate frequency with the time scale, V/l, results in a dimensionless frequency which remains constant at .027 throughout the Reynolds number range of 200 to 1300. This clearly shows that the hot-film probe is sensitive enough to detect even the slightest variations in the flow characteristics. By continuously recording and analyzing the temperature and the flow rate, we know which frequency, detected by the hot-film probe, corresponds to an actual flow fluctuation induced by hydrodynamic instability.

To make sure that the results are independent of the sampling rate, we collected the signals at 10 Hz and 100 Hz and compared the results. Since there were no differences between the two results, in all of our experiments, the temperature and flow rate signals are recorded at 10Hz, and the hot-film output is collected at 100 Hz.

We also investigated the possible dependence of the results on the location of the hot-film on the cavity wall. To ensure that the particular location of the probe does not influence the quantitative results, we made measurements at two different locations, one 12mm from the bottom wall and the other location, 4mm from the bottom. Several experiments were completed at each setting. The signals are statistically the same for both locations, showing no detectable difference in the results.

Figures 3a-g, the plots of the power spectrum from the hot-film anemometer, show the state and the frequency of the flow fluctuations. The abscissa is the frequency nondimensionalized with f*= V/d. At R=804, the flow is steady state (S). The small peaks at the low frequency range are due to slight fluctuations in temperature and flow rate. The small peak at .027 is due to the flow rate, as mentioned before.

At Reynolds number 935, a peak appears at $f_1 = 0.1122$, signaling the onset of a time periodic (TP) state. Comparing the power spectrum plots at R = 878, 935, and 966, it becomes clear that the small peak at ~.027, which remains virtually unchanged with R, is a small-amplitude external disturbance in the flow. The f_1 frequency, however, increases in strength with the Reynolds number until at R=992 a second peak appears at $f_2 = 0.00556$. Since f_2 is incommensurate with f_1, the flow is in a quasi-periodic (QP) state, indicating transition from a limit cycle to a torus. The second frequency, f_2, first appears as a small peak at R=966 and rapidly grows with R.

Our experiments show that the flow remains quasi-periodic up to R=1055, above which many other modes are exited until a broad band of frequencies appear. This state, we believe, is a low-dimensional chaotic state (U).

4. DISCUSSION AND CONCLUSIONS

The results of this study indicate that the transition to unsteady state in a lid-driven cavity with throughflow is via a torus bifurcation. Although we have only observed the sequence S-->TP-->QP-->U, there could be other periodic states that our experimental equipment is not sensitive enough to detect. We were careful to exclude any disturbances from external sources by monitoring all of the parameters which could influence the flow and the signal from the hot-film anemometer.

The disturbances due to the slow variations in temperature and flow rate were continuously measured during the experiments. Although these external fluctuations present small but finite-amplitude disturbances in the flow, we do not expect these disturbances to influence the results. To examine the nature of these transitions, we have decreased the Reynolds number and observed a reverse transition at about the same value where the forward transitions occur. This indicates that these are supercritical bifurcations and, therefore, immune to small-amplitude external disturbances. In other words, the bifurcations are generic and do not change qualitatively with small disturbances.

An advantage of using a hot-film anemometer is its capability to accurately detect the frequency of the flow fluctuations. Although with our previous flow visualization technique [3], we were able to correctly estimate the critical Reynolds number for transition to the time periodic state, we were unable to accurately measure the frequency of the flow fluctuations. As we have indicated before [3], the purpose of the flow visualization is mainly qualitative and could be misleading if over-extended to quantitative measurements.

The results presented here verify the critical Reynolds number reported previously for the transition to time periodic flow. Furthermore, our measurements show other transitions to a quasiperiodic state and finally a state with a broad band of frequencies. It appears that the transitions from steady state to unsteady state in this system are ordered, and the flow becomes chaotic through a torus bifurcation.

ACKNOWLEDGEMENTS

This research is supported by a grant from an industrial consortium through the Institute of Paper Science and Technology. Partial support for equipment is provided by Beloit Corporation. Portions of this work were used by JDB as partial fulfillment of the requirements for the M.S. degree at the School of Mechanical Engineering at Georgia Institute of Technology.

LIST OF FIGURES

REFERENCES

1. C.K. Aidun and N.G. Triantafillopoulos, "Global Stability Properties of Flow in the Pond of a Short Dwell Coater," *Int. Symp. Mech. Thin-Film Coating, Spring National Meeting of the AIChE*, March 18-22, 1990.

2. D. D. Heckelman Jr. and C.M. McC. Ettles. "Viscous and Inertial Pressure Effects at the Inlet to a Bearing Film," *STLE Transactions*, **31**, 1, 1988.

3. C.K. Aidun, N.G. Triantafillopoulos, and J. D. Benson, "Global Stability of a Lid-Driven Cavity with Throughflow," *Phys. Fluids* A **3** (9), 1991.

4a. J.R. Koseff and R.L. Street, "Visualization Studies of a Shear Driven Three-dimensional Recirculating Flow," *J. Fluid Eng.*, **106**, 21, 1984a.

4b. J.R. Koseff and R.L. Street, "On End Wall Effects in a Lid-Driven Cavity Flow," *J. Fluid Eng.* **106**, 385, 1984b.

4c. J.R. Koseff and R.L. Street, "The Lid-Driven Cavity Flow: A Synthesis of Qualitative and Quantitative Observations," *J. Fluid Eng.*, **106**, 390, 1984c.

5. A.K. Prasad and J.R. Koseff, "Reynolds Number and End-Wall Effects on a Lid-Driven Cavity Flow," *Phys. Fluids* A **1** (2), 208, 1989.

6. C.J. Freitas and R.L. Street, "Non-Linear Transient Phenomena in a Complex Recirculating Flow: A Numerical Investigation," *Int. J. Num. Methods in Fluids*, **8**, 769, 1988.

7. G. Comte-Bellot, "Hot Wire Anemometry," *Annual Review of Fluid Mechanics*, **8**, 209-31, 1976.

8. S.C. Ling and P.G. Hubbard, "The Hot-film Anemometer: A New Device for Fluid Mechanics Research," *J. of the Aeronautical Sciences*, **23**, 890-891, 1956.

9. L.M. Fingerson, "Parameter for Comparing Anemometer Response," *Paper presented at the Symposium on Turbulence in Liquids. University of Missouri-Rolla*, October 4-6, 1971.

10. J.D. Benson, M.S. Thesis, Georgia Institute of Technology, Atlanta, GA., "Transition to a Time-Periodic State in a Through-Flow Lid-Driven Cavity," 1991.

11. J.D. Benson and C.K. Aidun, "Transition to a Time-Periodic State in a Through-Flow Lid-Driven Cavity," *Bulletin of the American Physical Society*, **36** (10), 1991.

12. M.R. Davis, "The Dynamic Response of Constant Resistance Anemometers," *J. of Physics E: Scientific Instruments*, **3**, 15-20, 1970.

13. W. Tillmann and H. Schlieper, "A Device for the Calibration of Hot-Film Wall Shear Probes in Liquids," *J. of Physics E: Scientific Instruments*, **12**, 373-380, 1979.

14. W. Tillmann, M. Waschmann, M. Herold, and G. Häubinger, " Hot-film Wall Shear Probe for Measurement at Flexible Walls," *J. of Physics E: Scientific Instruments*, **14**, 692-694, 1981.

15. S. Nandy and J.M. Tarbell, "Flush-Mounted Hot Film Anemometer Accuracy in Pulsatile Flow," *J. Biomechanical Eng.*, **108**, 228-231, 1986.

16. H.L. Langhaar, "Steady Flow in the Transition Length of a Straight Tube," *J. of Applied Mechanics*, **9**, 55-58, 1942.

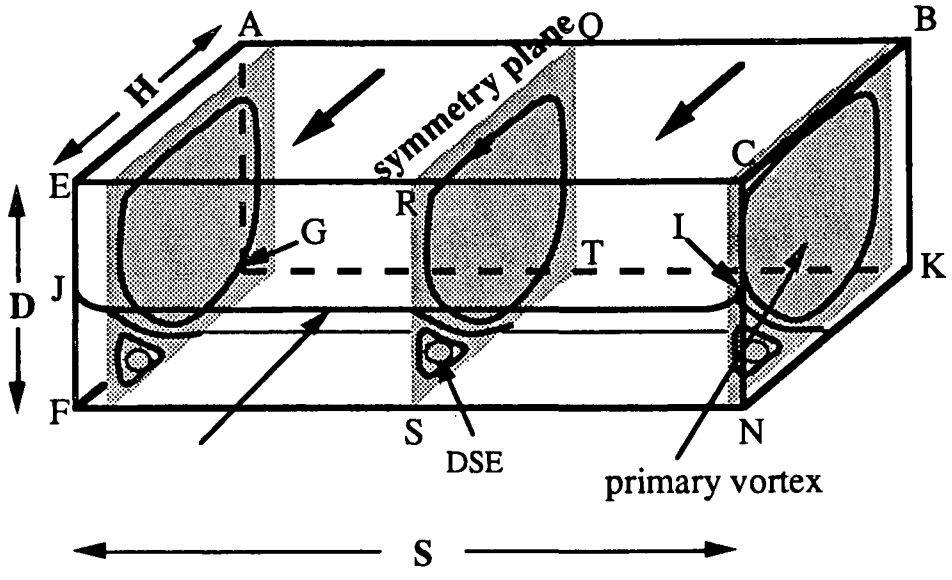

Figure 1 Schematic of the experimental setup and the rolled-shaped patterns of the steady state primary mode (S).

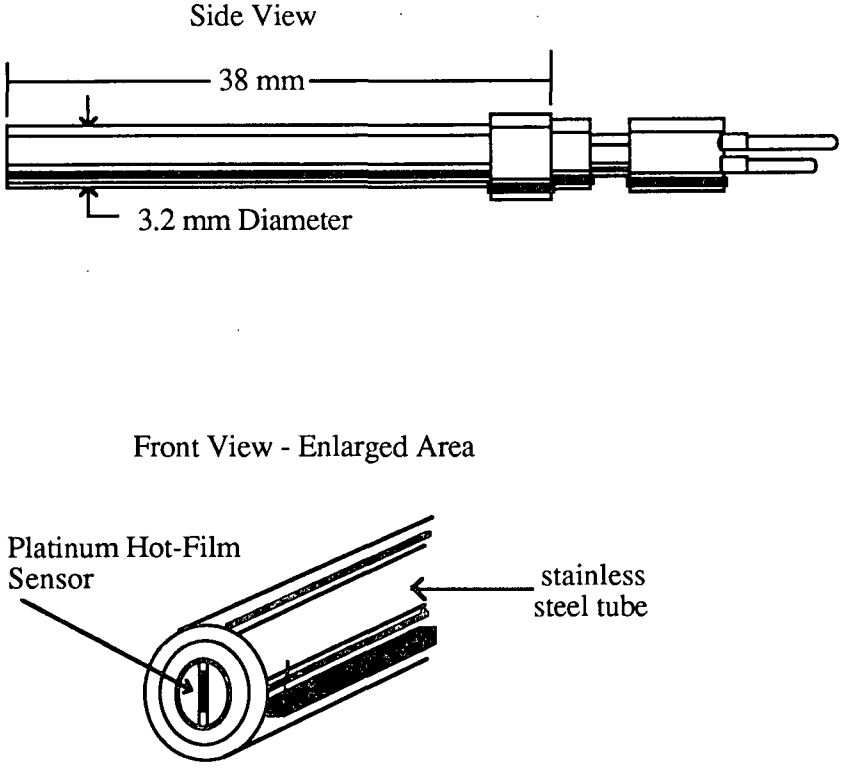

Figure 2 Schematic of a flush-mounted hot-film anemometer.

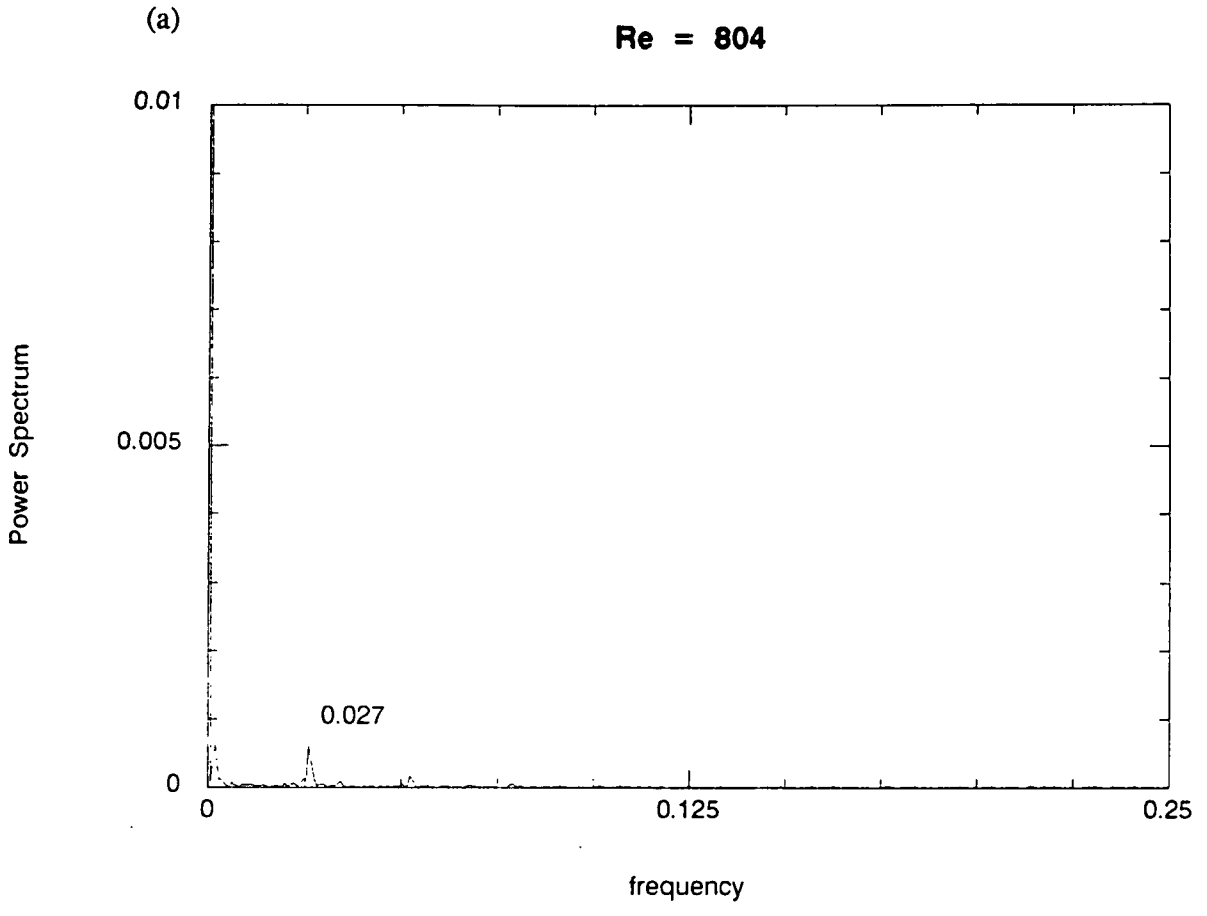

Figure 3a Power spectrum of the signal from the hot-film anemometer.

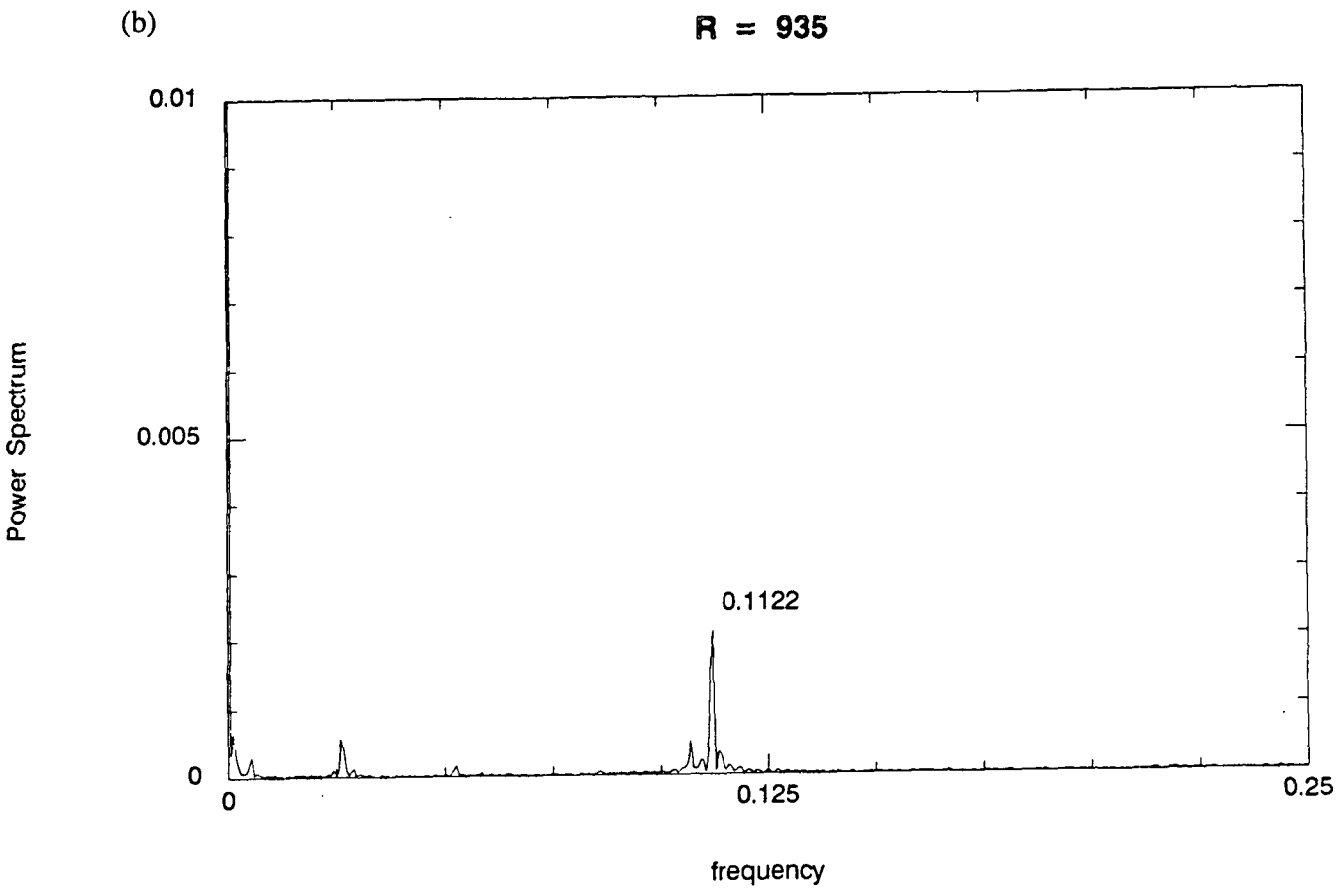

Figure 3b Power spectrum of the signal from the hot-film anemometer.

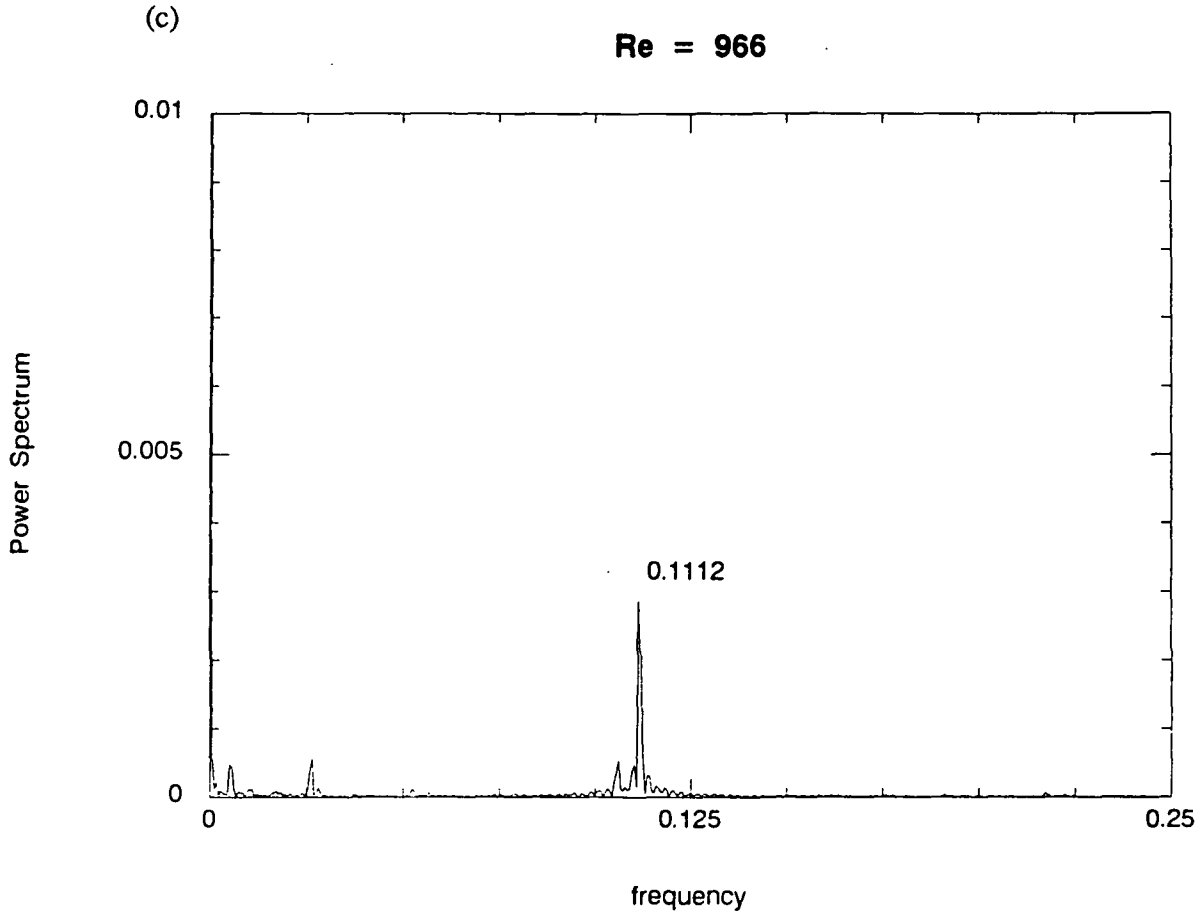

Figure 3c Power spectrum of the signal from the hot-film anemometer.

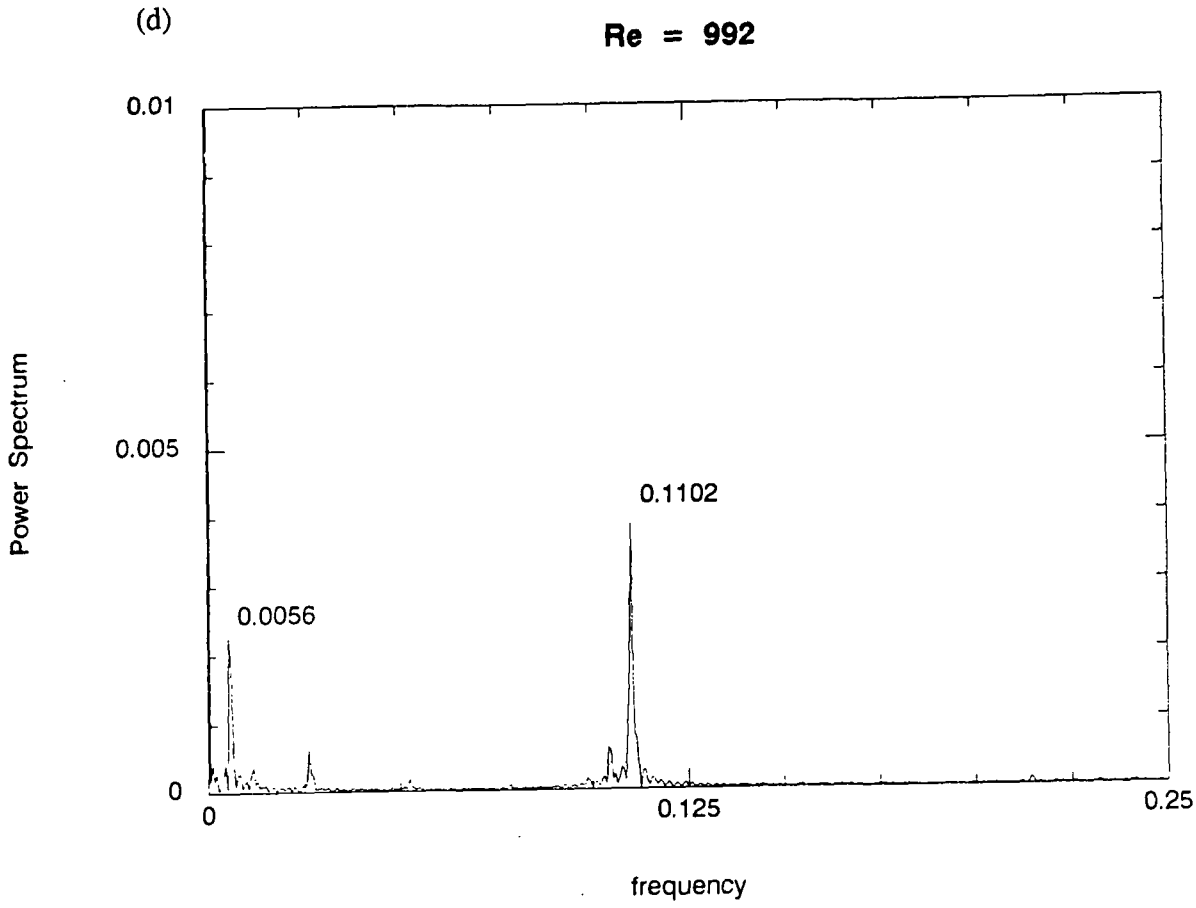

Figure 3d Power spectrum of the signal from the hot-film anemometer.

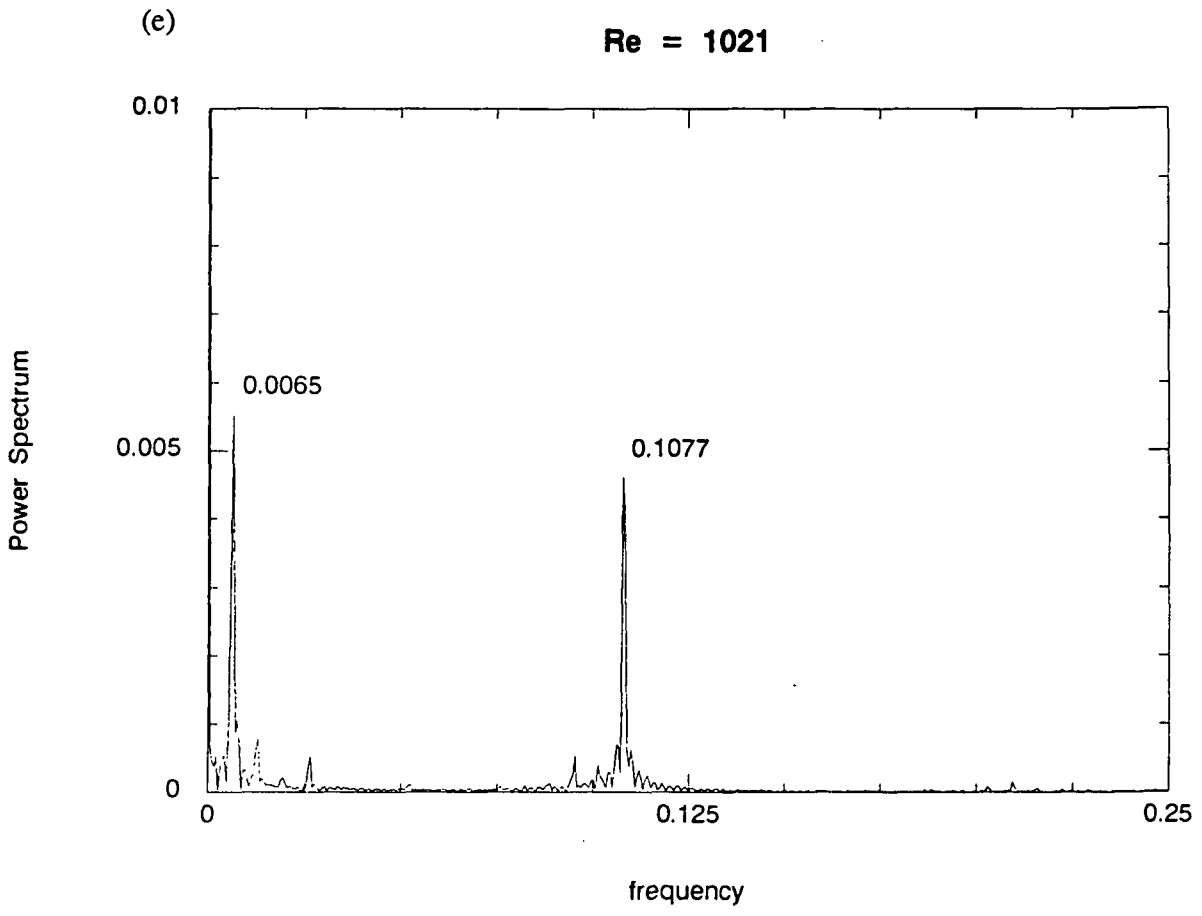

Figure 3e Power spectrum of the signal from the hot-film anemometer.

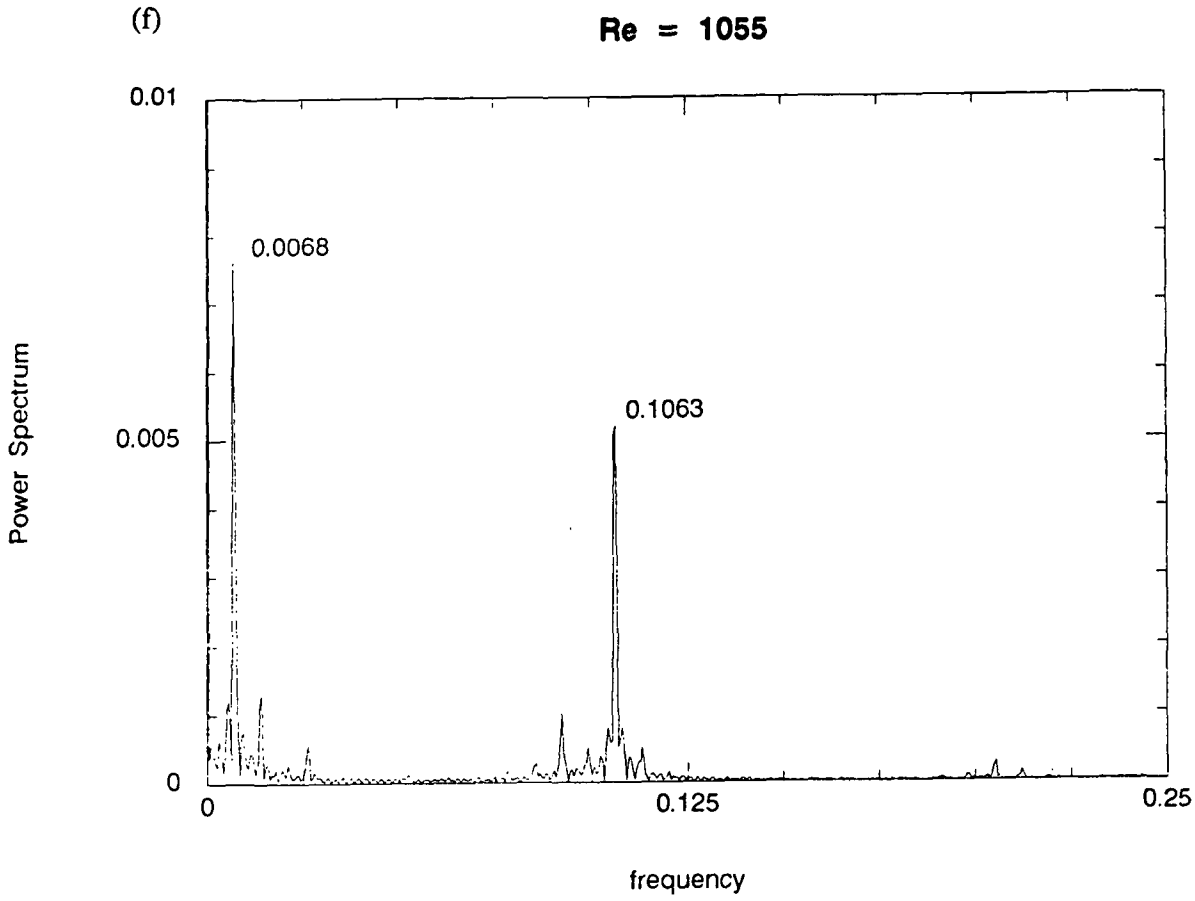

Figure 3f Power spectrum of the signal from the hot-film anemometer.

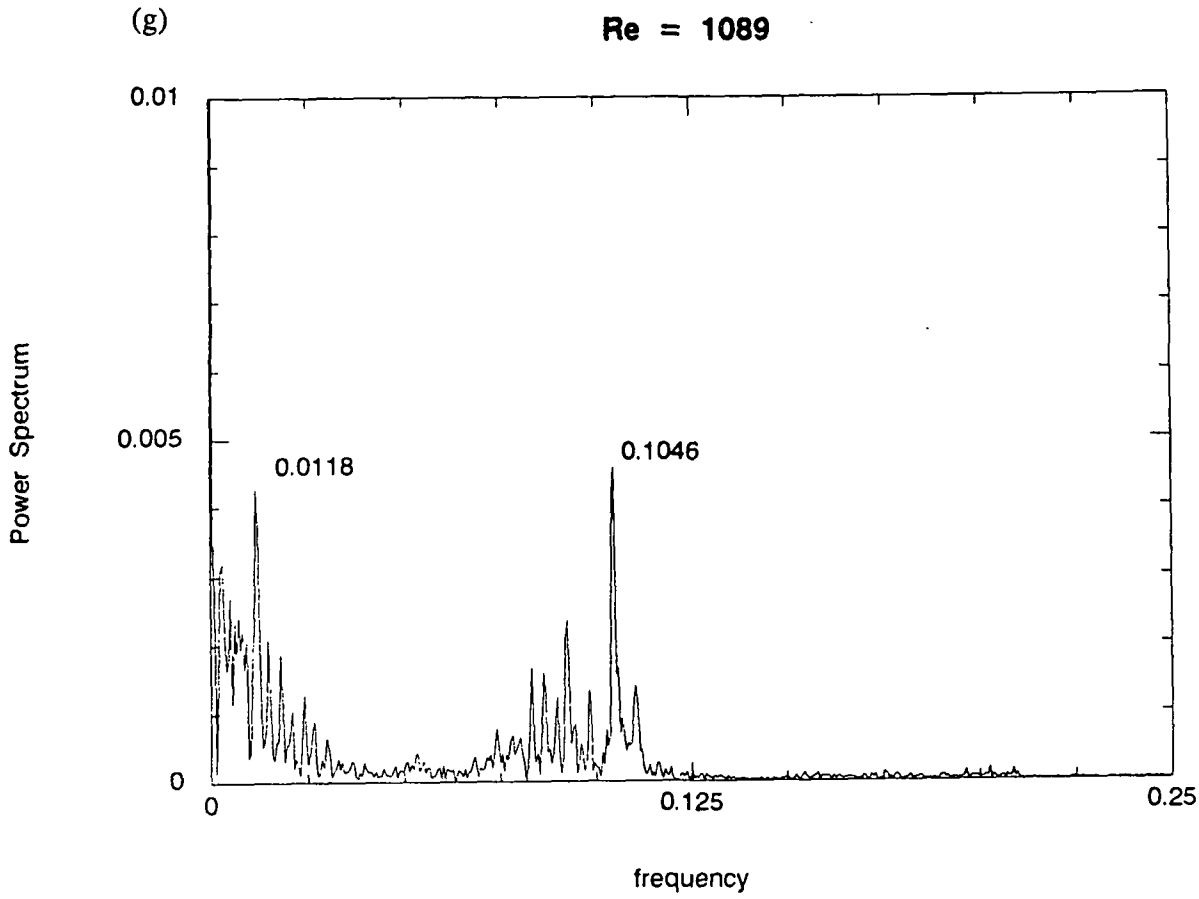

Figure 3g Power spectrum of the signal from the hot-film anemometer.